frontiers | Frontiers in Energy Research

TYPE Original Research
PUBLISHED 02 April 2024
DOI 10.3389/fenrg.2024.1378320

OPEN ACCESS

EDITED BY
Zhengmao Li,
Aalto University, Finland

REVIEWED BY
Bo Gu,
Sun Yat-sen University, China
Xiaoyan Wang,
Ibaraki University, Japan
Muhammad Adna,
National University of Computer and Emerging Sciences, Pakistan

*CORRESPONDENCE
Zhan Shi,
w_1234567892021@163.com

RECEIVED 29 January 2024
ACCEPTED 26 February 2024
PUBLISHED 02 April 2024

CITATION
Shi Z (2024), Delay and cost-balanced communication resource management for IoT-empowered distribution grid energy dispatch.
Front. Energy Res. 12:1378320.
doi: 10.3389/fenrg.2024.1378320

Delay and cost-balanced communication resource management for IoT-empowered distribution grid energy dispatch

Zhan Shi*

Guangdong Power Grid Co., Ltd., Power Dispatching Control Center, Communication Management Department, Guangdong, China

The combination of internet of things (IoT), 5G, and power line communication (PLC) provides real-time and low-cost data transmission services to meet the quality of service (QoS) requirements for distribution grid energy dispatch. However, the IoT-empowered communication resource management system faces challenges in optimizing delay and traffic cost for distribution grid energy dispatch. There is a contradiction between the long-term performance guarantee and short-term optimization objectives, compounded by competition for communication resources. In this paper, we construct the minimization problem of the weighted sum of data transmission delay and traffic cost. Utilizing Lyapunov optimization, we aim to decouple the long-term constraint of average queuing delay with the short-term optimization objective. Then, a delay and cost-balanced communication resource management algorithm based on two-layer iterative matching is proposed. It optimizes the communication mode selection by 1-to-2 bidding matching in a large timescale and subchannel allocation by many-to-many deferred acceptance matching in a small timescale. The simulation data present that the proposed algorithm excels in reducing data transmission delay, minimizing traffic cost, and decreasing queuing delay.

KEYWORDS

IoT, distribution grid energy dispatch, two-layer iterative matching, multi-timescale optimization, communication resource management, balance of delay and cost

1 Introduction

The internet of things (IoT) has a broad development prospect in the field of distribution grid energy dispatch. By connecting distribution grid operators with energy users and electric equipment (Tariq et al., 2020; Liao et al., 2023a; Fizza et al., 2023; Liu et al., 2023; Safdar Malik et al., 2023; Zhu et al., 2024), IoT provides dynamic data acquisition and real-time state perception of key electric equipment. Then, these collected data can be uploaded to the edge server or cloud server for deep state analysis and intelligent energy dispatch (Wang et al., 2023; Yao et al., 2023). Among various communication technologies, fiber optic technology cannot adapt to the wide coverage requirement of IoT due to the high deployment cost (Chagnon, 2019; Liao et al., 2023b; Lin et al., 2023). Wireless fidelity (WiFi) relying on the industrial, scientific, and medical (ISM) band is susceptible to interference and privacy issues (Schwung et al., 2023). In comparison, 5G and power line communication (PLC) emerge as feasible candidates (López et al., 2019; Pal et al., 2021; Zhou et al., 2022). Coverage by using a dedicated frequency band, but it causes extra traffic costs for

grid operators (Qian et al., 2022; Zhou et al., 2024; Zhou et al., 2023a). On the other hand, PLC has the advantages of low cost and flexible development, but it suffers from lower communication capacity. How to combine 5G and PLC to support the real-time energy dispatch of the distribution grid from a delay and cost balance perspective remains an open issue (Xu et al., 2021; Zhang et al., 2023; Ruby et al., 2023).

Communication resource management refers to the effective and reasonable configuration, monitoring, scheduling, and optimization of various resources of communication systems to meet the quality of service (QoS) requirements (Guo et al., 2021; Ding et al., 2022; Gu et al., 2022; Wang et al., 2023). When combining 5G and PLC with IoT, communication mode selection and subchannel allocation are two important research topics of communication resource management. Particularly, communication mode selection should be optimized in a large timescale because the frequently switching communication mode results in large overheads. On the other hand, subchannel allocation should be optimized in a small timescale, considering the temporal-varying characteristics of the channel state (Xiang et al., 2022; Bigdeli et al., 2023). Despite the great research efforts initiated by previous studies, how to realize scalable, reliable, stable, and adaptable communication resource management still faces several technical challenges.

First, the optimization of data transmission delay and traffic cost is contradictory to each other. Although 5G has lower latency, it significantly increases the total traffic cost, particularly under the scenario of second-level data collection (Gu et al., 2021). The switching between 5G and PLC should be dynamically adjusted in accordance with various parameters including delay, traffic cost, and channel quality. Second, severe competition for communication resources is inevitable when the number of IoT devices is overwhelming. The small-timescale subchannel allocation optimization of a device is not only affected by the large-timescale mode selection results but also related to decisions of other competing devices. This incurs further difficulty in the multi-timescale resource management problem (Leng et al., 2023). Finally, short-term optimization based on information lacking foresight leads to long-term performance deterioration. The long-term queuing delay requirement imposed by real-time energy dispatch is considered an example. The optimum policy to balance delay and cost may come at the expense of larger cumulative queue backlog, which deteriorates the long-term queuing delay performance (Huang et al., 2023).

There exist several studies on subchannel allocation in IoT. Zhou et al. (2020) launched an algorithm based on online learning, utilizing the context-aware multi-armed bandit framework to dynamically distribute channels in a 5G network, which has shown exceptional performance, particularly in large-scale network scenarios. Ning et al. (2019) proposed a blended framework for computational task offloading, designed to enhance real-time traffic handling within 5G network infrastructures. The goal is to maximize the sum offloading rate. Do and Lehnert (2011) proposed a PLC channel allocation protocol that considers the individual channel quality of each user, enabling precise calculations for the required transmission resources. Han et al. (2023) investigated an advanced channel allocation strategy involving dynamic two-step random access optimization to enhance the access success probability. Wang et al. (2018) proposed an innovative algorithm for joint power and channel allocation, with the objective of maximizing the sum rate for cellular users. However, these works overlook severe competition for communication resources caused by massive IoT devices. Dewa et al. (2021) proposed a distributed channel assignment algorithm that efficiently finds the optimal channel configuration using the concept of belief propagation. Li et al. (2023) proposed a multi-agent device-to-device (D2D) communication resource allocation algorithm based on the advantage actor critic (A2C) to dynamically and adaptively output the resource allocation scheme of D2D users. However, these works overlook severe competition for communication resources caused by massive IoT devices. The developed optimization approaches have the disadvantages of high complexity, slow convergence, and instability under resource competition.

Matching theory provides a feasible tool to address combinatorial optimization problems involving large-number participants. Meshgi et al. (2017) studied the channel allocation problem of multi-user multi-channel cellular networks and proposed a channel allocation scheme based on stable matching to effectively improve the system capacity. Islam et al. (2016) proposed a channel allocation method based on stable matching to effectively reduce delay and improve system throughput for D2D communications underlying cellular networks. Csercsik and Jorswieck (2023) proposed a novel preallocation-based combinatorial auction approach to optimize the efficient allocation of channels for ultra-reliable low-latency communication (URLLC) services. Zhou et al. (2021) considered priority-aware resource coordination in a multi-unmanned aerial vehicle (UAV) communication system and jointly optimized a channel assignment and power allocation strategy under stringent resource availability constraints. These works simply assume all the resources are optimized in the same timescale and cannot be applicable to our scenario involving large-timescale communication mode selection and small-timescale subchannel allocation. Huang et al. (2015) proposed a multi-timescale matching model to enhance the matching degree between the available wind supply and the increasing EV charging demand within the microgrid. Huang et al. (2015) and Yu et al. proposed an innovative algorithm aimed at addressing challenges in resource allocation and task division within non-orthogonal multiple access edge computing-based power IoT. Wang et al. (2021) proposed a low-complexity algorithm to solve the formulated subchannel allocation problem using the matching theory, where the joint optimization of the task assignment and power allocation is performed at each iteration. Huang et al. (2022) proposed a beacon synchronization-based multi-channel dynamic time slot assignment method. The channel is allocated based on interference minimization from adjacent channels. However, these studies ignore the coupling between the long-term queuing delay guarantee with the short-term optimization of delay and cost balance.

Thus, we design a delay and cost-balanced communication resource management framework for IoT-empowered distribution grid energy dispatch. First, we present models of delay and traffic cost and formulate a delay and traffic cost optimization problem. The optimization objective is to minimize the weighted sum of transmission delay and traffic cost under the constraints of the subchannel allocation number, subchannel allocation quota, data

transmission reliability, and long-term average queuing delay. Then, we decompose the formulated problem into two main subproblems, i.e., a large-timescale subproblem involving device communication mode selection and a small-timescale subproblem focusing on subchannel allocation, and solve them alternatively by the proposed delay and cost-balanced communication resource management algorithm based on two-layer iterative matching. The specific contributions include the following.

- Communication resource management with delay and traffic cost balancing: The proposed algorithm dynamically adjusts the optimization policy to trade off data transmission delay with traffic cost, which is an oversight in related works.
- Communication resource competition solution and complexity reduction: At each epoch, the large-timescale mode selection problem is addressed through the utilization of I-to-2 bidding matching. The small-timescale subchannel allocation problem is solved based on many-to-many deferred acceptance matching at each slot. This multi-timescale matching improves the convergence speed and complexity performances and the overheads caused by frequent switching in related works.
- Guarantee of long-term queuing delay: Based on Lyapunov optimization, we transform the long-term queuing delay constraint into a virtual queue. Then, the product of the virtual queue backlog and the queuing delay is added into the optimization objective. Particularly, devices with large queue backlog and queuing delay are given priority in matching so as to realize long-term queuing delay guarantee, which is a lack of consideration in related works.

The remainder of this paper is structured in the subsequent manner: An exposition of the system model and the formulation of the problem are explained in Section 2. The algorithm proposed, which relies on a two-tiered iterative matching process, is elucidated in Section 3. Section 4 is dedicated to demonstrating the outcomes derived from simulations. The conclusion of this study is presented in Section 5. The notations used in this paper are summarized in Table 1.

2 System model

Figure 1 introduces the proposed delay and cost-balanced communication resource management framework for IoT-empowered distribution energy dispatch, which includes the device layer, transmission layer, and edge layer. In the device layer, I IoT devices which support both PLC and 5G communication modes are deployed on electrical equipment including distributed photovoltaic, energy storage unit, power distribution equipment, and electrical vehicle charging pile to collect various types of data such as active power, reactive power, and temperature (Adnan et al., 2019; Ali et al., 2021). Define the set of IoT devices as $\mathcal{M} = \{m_1, \ldots, m_i, \ldots, m_I\}$. The transmission layer contains a PLC gateway and a 5G base station for data transmission, which support dual communication modes, i.e., PLC and 5G. An orthogonal frequency division multiplexing (OFDM)-based data transmission scheme is adopted. There exist J orthogonal subchannels, including J_1 PLC subchannels and J_2 5G subchannels. Define the set of subchannels as $\mathcal{N} = \{n_1, \ldots, n_j, \ldots, n_J\}$, where $n_j, j = 1, \ldots, J_1$ are PLC subchannels, and $n_j, j = J_1 + 1, \ldots, J$ are 5G subchannels. The data collected by IoT devices are uploaded to the edge layer via a selected communication mode and allocated subchannels, i.e., either PLC subchannels or 5G subchannels. The edge layer contains an edge server that processes the data uploaded from the device layer. The edge server also optimizes communication resource management in terms of communication mode selection and subchannel allocation.

Device communication mode selection and subchannel allocation are optimized in different timescales. Particularly, to avoid frequent switching of the communication mode and reduce overheads, in a large timescale, i.e., epoch, mode selection is optimized, while in a small timescale, i.e., time slot, subchannel allocation is optimized (Sezer and Gezici, 2016; Yu et al., 2021; Li et al., 2023; Zhou et al., 2023b). We consider a duration which contains T slots. Each slot lasts a duration τ. Define the slot's set as $\mathcal{T} = \{1, \ldots, t, \ldots, T\}$ and the epoch's set as $\mathcal{V} = \{1, \ldots, v, \ldots, V\}$. Each epoch contains consecutive T_0 slots. The relationship between V and T satisfies $T = T_0 V$. The slot's set in the v-th epoch is denoted as $\mathcal{T}(v) = \{(v-1)T_0 + 1, (v-1)T_0 + 2, \ldots, vT_0\}$.

Define $\boldsymbol{x}_i(v) = \left\{x_i^{\mathrm{PLC}}(v), x_i^{\mathrm{5G}}(v)\right\}$ as the set of optimization variables of large timescale device communication mode selection, where $x_i^{PLC}(v)$ and $x_i^{5G}(v)$ are the indicator variables of the 5G communication mode and PLC mode, respectively. $x_i^{\mathrm{PLC}}(v) = 1$ indicates that device m_i selects the PLC mode to upload data to the edge server in the v-th epoch; otherwise, $x_i^{\mathrm{PLC}}(v) = 0$. Similarly, $x_i^{\mathrm{5G}}(v) = 1$ indicates that device m_i selects the 5G communication mode, and otherwise $x_i^{\mathrm{5G}}(v) = 0$. Define $y_{i,j}(t)$ as the optimization variable of small-timescale subchannel allocation. $y_{i,j}(t) = 1$ indicates that in the t-th slot, the edge server allocates subchannel n_j to device m_i, and otherwise, $y_{i,j}(t) = 0$. Denote q_m as the quota of subchannel allocation, i.e., at most q_m subchannels can be allocated for each device per slot. Meanwhile, due to the limited number of subchannels in each communication mode, PLC subchannels can be allocated to at most J_1 devices, and 5G subchannels can be allocated to at most J_2 devices.

2.1 Data transmission model

In the t-th slot, the data transmission rate for device m_i on subchannel n_j is calculated as

$$R_{i,j}(t) = N_s \min\left(R_j^{\max}, \left\lfloor \log_2\left(1 + \frac{P_{i,j}(t)\, g_{i,j}(t)}{\Gamma_i}\right)\right\rfloor\right), \tag{1}$$

where $\lfloor \cdot \rfloor$ represents that the number is rounded down to the nearest integer. N_s is the OFDM symbol rate. $R_j^{\max}$ (bits/symbol) is the maximum transmitted bits per symbol for subchannel n_j, which is determined based on the modulation method, signal-to-noise ratio, frequency selective fading, computational complexity, and other factors to guarantee signal quality. Γ_i is the signal-to-interference-plus-noise ratio (SINR) gap coefficient, and $g_{i,j}(t)$ is the subchannel gain, which are calculated as

$$\Gamma_i \approx \frac{\left[Q^{-1}(P_e/4)\right]^2}{3}, \tag{2}$$

$$g_{i,j}(t) = \frac{|H_{i,j}(t)|^2}{N_j^{\mathrm{EMI}}(t) + N_0}, \tag{3}$$

TABLE 1 Summary of notations.

Notation	Definition	Notation	Definition
I	Number of IoT devices	$\mathcal{M}$	Set of IoT devices
J	Number of orthogonal subchannels	J_1	Number of PLC subchannels
J_2	Number of 5G subchannels	$\mathcal{N}$	Set of subchannels
T	Number of slots	τ	Slot duration
$\mathcal{T}$	Set of slot	V	Epoch
$\mathcal{V}$	Set of epoch	$\boldsymbol{x}_i(v)$	Set of communication mode selection optimization variables
$x_i^{\mathrm{PLC}}(v)$	PLC mode variable	$x_i^{5\mathrm{G}}(v)$	5G communication mode variable
$y_{i,j}(t)$	Subchannel allocation variable	$q+m$	Quota of subchannel allocation
$R_{i,j}(t)$	Data transmission rate	N_s	OFDM symbol rate
$R_j^{\max}$	Maximum transmitted bits per symbol for the subchannel	Γ_i	SINR gap coefficient
$g_{i,j}(t)$	Subchannel gain	P_e	Target bit error rate
$H_{i,j}(t)$	Frequency response of device $m_i$on the subchannel n_j	N_0	Gaussian noise
$N_j^{\mathrm{EMI}}(t)$	Electromagnetic interference	lg$f(x)$	Electromagnetic interference characteristic function
v	Characteristic index	η	Skewed parameter
μ	Positional parameter	θ	Scale parameter
$SINR_{i,j}(t)$	SINR of device $m_i$on subchannel n_j	$SINR_{\min}$	Lower bound of SINR
$L_i(t)$	Backlog of the device-side data queue	$A_i(t)$	m_i's collected data amount
$D_i(t)$	m_i's throughput	$\tau_i(t)$	Data transmission delay from $m_i$to the edge server
$C_i(t)$	Extra traffic cost	$e^{5\mathrm{G}}(v)$	Unit cost of transmitting single-bit data through the 5G subchannel
$\tau_i^{\mathrm{que}}(t)$	Queuing delay of data transmission	$\widehat{A}_i(t)$	Average data arrival rate of m_i
$\tau_{i,\max}^{\mathrm{que}}$	Average queuing delay threshold	α	Weight of traffic cost
$O_i(t)$	Virtual queue of the constraint of long-term average queuing delay	$\gamma_i^{\mathrm{PLC}}(v)$, $\gamma_i^{5\mathrm{G}}(v)$	Preference values of device $m_i$for selecting PLC and 5G communication mode
$p_i^{\mathrm{PLC}}(v)$, $p_i^{5\mathrm{G}}(v)$	Bidding prices for device $m_i$to select PLC and 5G communication mode	$\mathbf{\Pi}$	Set of devices queuing for matching
$\mathbf{\Lambda}^{\mathrm{PLC}}$, $\mathbf{\Lambda}^{5G}$	Set of devices that issue requests to PLC and 5G communication mode	ρ	Predefined constant
β^{PLC}, $\beta^{5\mathrm{G}}$	Bidding price coefficients for the PLC and 5G communication modes	$\Theta_i(t)$	Set of PLC subchannels that are currently matched with m_i
$\lvert\Theta_i(t)\rvert$	Size of $\Theta_i(t)$	$\omega_{i,j}(t)$	Reciprocal of the data transmission delay
$\lambda_{i,j}(t)$	Product of the virtual queue backlog and queuing delay	$\mathcal{N}_i(t)$	Set of available 5G subchannels for m_i
$\mathcal{F}_i^D$	Partial preference list of 5G subchannels	$\mathcal{F}_j^C$	Partial preference list of the subchannel n_j

where P_e is the target bit error rate. $Q^{-1}(\cdot)$ is the inverse function of $Q(x)=\frac{1}{2\pi}\int_x^{\infty}e^{t^2/2}dt$. $H_{i,j}(t)$ is the frequency response of device m_i on subchannel n_j. N_0 is Gaussian noise. $N_j^{\mathrm{EMI}}(t)$ is the electromagnetic interference generated by the operation of the electrical equipment. We use the alpha steady-state function to describe electromagnetic interference (Zhou et al., 2016), and its characteristic function is

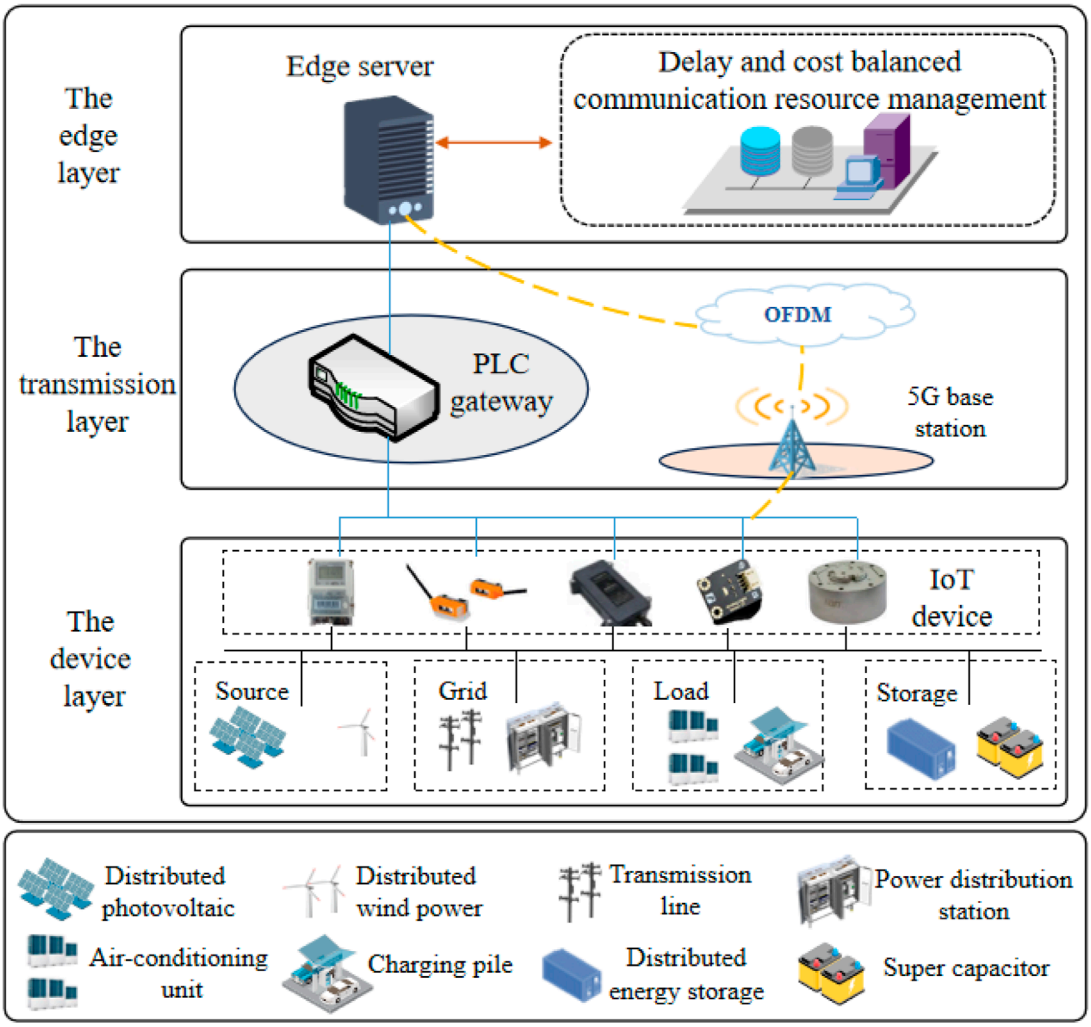

FIGURE 1
Delay and cost-balanced communication resource management framework for IoT-empowered distribution energy dispatch.

given by

$$\lg f(x) = \begin{cases} -\theta^{v}|x|^{v}\left[1 - j\eta \operatorname{sign}(x)\tan\frac{\pi v}{2}\right] + j\mu x & , v \neq 1 \\ -\theta|x|\left[1 - j\eta \operatorname{sign}(x)\frac{2}{\pi}\lg|x|\right] + j\mu x & , v = 1 \end{cases}, \quad (4)$$

where $v \in (0,2)$ is the characteristic index. $\eta \in [-1,1]$ is a skewed parameter that determines the slope. $\theta > 0$ is a scale parameter used to measure the dispersion. $\mu \in \mathbf{R}$ is a positional parameter. When $v \in (1,2]$, μ represents the average value; when $v \in (0,1]$, μ represents the median. sign(·) is the sign function.

Define the SINR of device m_i on subchannel n_j as

$$SINR_{i,j}(t) = \frac{P_{i,j}(t)g_{i,j}(t)}{\Gamma_i}. \quad (5)$$

To ensure reliable data transmission, the SINR constraint is given by

$$SINR_{i,j}(t) \geq SINR_{\min}, \quad (6)$$

where $SINR_{\min}$ represents the lower bound of SINR.

2.2 Transmission delay and the traffic cost model

The data stored at m_i is modeled as a device-side data queue, the backlog of which evolves as

$$L_i(t+1) = L_i(t) + A_i(t) - D_i(t), \quad (7)$$

where $A_i(t)$ is m_i's collected data amount in the t-th slot. $D_i(t)$ is m_i's throughput, i.e., the amount of data leaving $L_i(t)$, which is calculated as

$$D_i(t) = \min\left\{L_i(t) + A_i(t), \tau\sum_{j=1}^{J} y_{i,j}(t)R_{i,j}(t)\right\}. \quad (8)$$

Therefore, in the t-th slot, the data transmission delay from m_i to the edge server is given by

$$\tau_i(t) = \min\left\{\tau, \frac{L_i(t) + A_i(t)}{\sum_{j=1}^{J} R_{i,j}(t)}\right\}. \quad (9)$$

Since the PLC network belongs to the power grid assets, there is no additional traffic cost when using PLC for data transmission. On the other hand, although 5G provides a higher transmission rate, it belongs to the assets of the telecommunication operator. Extra traffic cost is required when using 5G for data transmission, which is given by

$$C_i(t) = x_i^{5G}(v)\, e^{5G}(v)\, D_i(t), \tag{10}$$

where $e^{5G}(v)$ represents the unit cost of transmitting single bit data through the 5G subchannel at the v-th epoch.

2.3 Queuing delay model

For the data queue, we normally expect the mean rate of data queue to be stable. $L_i(t)$ is mean rate stable if

$$\lim_{T\to\infty} \frac{\mathbb{E}\{|L_i(t)|\}}{T} = 0. \tag{11}$$

Queuing delay is defined as the ratio obtained by dividing the average quantity of data backlogged in the queue by the mean rate at which data arrive. Then, the queuing delay of data transmission at device m_i is given by

$$\tau_i^{que}(t) = \frac{L_i(t)}{\widehat{A}_i(t)}, \tag{12}$$

where $\widehat{A}_i(t)$ is the average data arrival rate of m_i, which is calculated as

$$\widehat{A}_i(t) = \frac{1}{t-1}\sum_{s=1}^{t-1} A_i(s). \tag{13}$$

To avoid a large queue backlog and meet the low-delay requirement of energy dispatch, a constraint of the long-term average queuing delay over T slots is given by

$$\lim_{T\to\infty} \frac{1}{T}\sum_{t=1}^{T} \tau_i^{que}(t) \le \tau_{i,\max}^{que}, \tag{14}$$

where $\tau_{i,\max}^{que}$ represents the average queuing delay threshold.

2.4 Problem formulation

The optimization problem is a joint minimization problem that aims to jointly minimize data transmission delay and traffic cost through the large-timescale optimization of device communication mode selection and the small-timescale optimization of subchannel allocation. The constraints of the subchannel allocation number, subchannel allocation quota, data transmission reliability, and long-term average queuing delay are taken into account. The data transmission delay and traffic cost joint minimization problem is formulated as

$$\begin{aligned}
\mathbf{P1}: \min_{\{\boldsymbol{x}_i(v), y_{i,j}(t)\}} \lim_{T\to\infty} \frac{1}{T}\sum_{t=1}^{T}\sum_{i=1}^{I}\left[\tau_i(t) + \alpha C_i(t)\right] \\
\text{s.t.}\quad C_1: x_i^{PLC}(v), x_i^{5G}(v) \in \{0,1\}, \forall m_i \in \mathcal{M}, \forall v \in \mathcal{V}, \\
C_2: x_i^{PLC}(v) + x_i^{5G}(v) = 1, \forall m_i \in \mathcal{M}, \forall v \in \mathcal{V}, \\
C_3: \ 0 \le \sum_{i=1}^{I} x_i^{PLC}(v) \le J_1, \forall v \in \mathcal{V}, \\
C_4: 0 \le \sum_{i=1}^{I} x_i^{5G}(v) \le J_2, \forall v \in \mathcal{V}, \\
C_5: \ 0 \le \sum_{j=1}^{J}\left[x_i^{PLC}(v) y_{i,j}(t) + x_i^{5G}(v) y_{i,j}(t)\right] \\
\quad \le q_m, \forall m_i \in \mathcal{M}, \forall t \in \mathcal{T}, \forall v \in \mathcal{V} \\
C_6: \sum_{i=1}^{I}\left[x_i^{PLC}(v) y_{i,j}(t) + x_i^{5G}(v) y_{i,j}(t)\right] \\
\quad \le 1, \forall n_j \in \mathcal{N}, \forall t \in \mathcal{T}, \forall v \in \mathcal{V} \\
C_7: \ SINR_{i,j}(t) \ge SINR_{\min}, \forall m_i \in \mathcal{M}, \forall n_j \in \mathcal{N}, \forall t \in \mathcal{T}, \\
C_8: \lim_{T\to\infty} \frac{1}{T}\sum_{t=1}^{T} \tau_i^{que}(t) \le \tau_{i,\max}^{que},
\end{aligned} \tag{15}$$

where α represents the weight of traffic cost. C_1 is the constraint of the large-timescale device communication mode selection variable. C_2 indicates that the device can only choose one of the communication modes in an epoch. C_3 indicates that PLC channels can be allocated to at most J_1 devices. C_4 indicates that 5G subchannels can be allocated to at most J_2 devices. C_5 is the constraint on the number of subchannels allocated to one device in each slot. C_6 indicates that each subchannel can be allocated to at most one device. C_7 is the constraint of the data transmission reliability requirement. C_8 is the constraint of long-term average queuing delay.

2.5 Problem transformation

The formulated joint optimization problem is a stochastic problem with a long-term perspective, which cannot be solved in polynomial time because the long-term constraint of average queuing delay is coupled with the short-term tradeoff between queuing delay and traffic cost per slot. Therefore, we utilize Lyapunov optimization to provide a tractable solution by transforming the problem based on the virtual queue concept. Specifically, virtual queue $O_i(t)$ corresponding to C_8 evolves as

$$O_i(t+1) = \max\left\{O_i(t) + \tau_i^{que}(t) - \tau_{i,\max}^{que}, 0\right\}. \tag{16}$$

If $O_i(t)$ is mean rate stable, C_8 holds automatically. Based on $O_i(t)$, **P1** is rewritten as

$$\begin{aligned}
\mathbf{P2}: \min_{\{\boldsymbol{x}_i(v), y_{i,j}(t)\}} \sum_{i=1}^{I}\left[\tau_i(t) + \alpha C_i(t) + O_i(t)\tau_i^{que}(t)\right] \\
\text{s.t.}\quad C_1 \sim C_7.
\end{aligned} \tag{17}$$

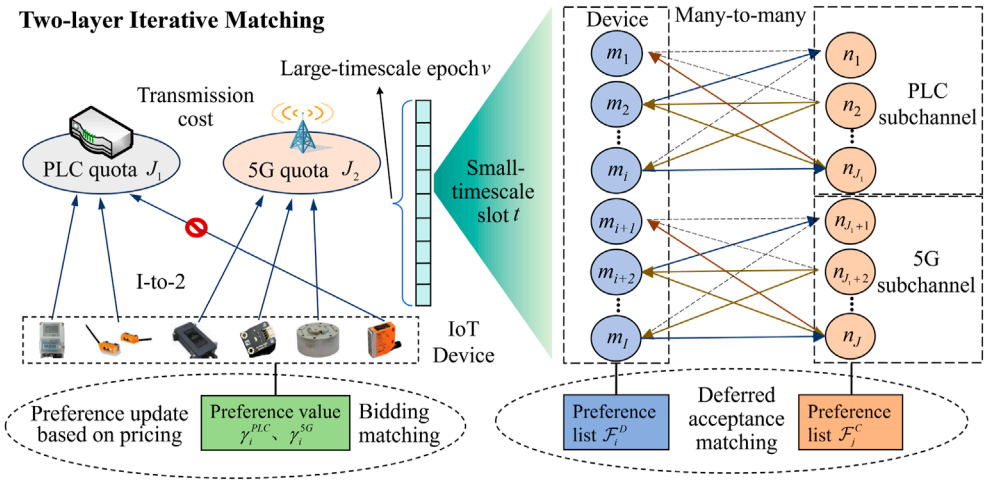

FIGURE 2
Schematic diagram of the delay and cost-balanced communication resource management algorithm based on two-layer iterative matching.

3 Delay and cost-balanced communication resource management algorithm based on two-layer iterative matching

The optimization problem formulated in (17) involves both large and small timescales. To address it, we propose a delay and cost balanced communication resource management algorithm based on two-layer iterative matching, which is shown in Figure 2. First, the initial optimization problem has been broken down into a communication mode selection subproblem in large-timescale epoch and a subchannel allocation subproblem in a small-timescale slot. Next, we propose a large-timescale communication mode selection algorithm based on *I*-to-2 bidding matching to select the communication mode at each epoch. Here, *I*-to-2 indicates that the matching is implemented in a bidding fashion between I devices and two communication modes. On this basis, based on the many-to-many deferred acceptance matching algorithm, a small-timescale subchannel allocation algorithm is proposed to match devices with subchannels based on bilateral preferences.

3.1 Large-timescale communication mode selection based on I-to-2 bidding matching

In this subsection, the proposed large-timescale communication mode selection algorithm based on *I*-to-2 bidding matching is introduced. It establishes a stable matching between I devices and two communication modes through iterative bidding. As the communication mode selected by a device in a large-timescale epoch influences the data transmission delay and traffic cost of multiple slots in that epoch, the large-timescale decision-making is coupled with future performance of small-timescale optimization. To address the issue of the lack of a priori knowledge of future performance, historical data transmission delay and historical traffic cost are used to construct the preference value of device toward the communication mode. Then, a device selects its most preferred communication mode based on the preference values.

However, due to the constraint of the subchannel number, matching competition among devices occurs if the device number selecting the PLC mode exceeds J_1, or the device number selecting the 5G communication mode exceeds J_2. Bidding matching can effectively solve the competition between devices, improve the convergence speed, and reduce the complexity by lowering the preference value so as to enforce devices giving up competing for the same communication mode. The proposed algorithm adopts iterative bidding to resolve competition among devices toward communication mode selection. Specifically, a bidding price is introduced to reduce the preference value of a device toward the competing communication mode at each iteration, thereby forcing some devices to choose the other communication mode and quit competition. Moreover, the bidding price can be dynamically adjusted according to the virtual queue backlog and queuing delay to provide higher priority for devices with a larger queue backlog and queuing delay. The specific implementation procedures are summarized in Algorithm 1, which are introduced below.

3.1.1 Initialization

Define the preference values of device m_i for selecting the PLC mode and 5G communication mode as $\gamma_i^{\mathrm{PLC}}(v)$ and $\gamma_i^{5G}(v)$, respectively. The bidding prices for device m_i to select the PLC mode or 5G communication mode are defined as $p_i^{\mathrm{PLC}}(v)$ and $p_i^{5G}(v)$.

Represent the set of devices queuing for matching as $\mathbf{\Pi}$, the set of devices that issue requests to PLC mode as $\mathbf{\Lambda}^{\mathrm{PLC}}$, and the set of devices that issue requests to 5G communication mode as $\mathbf{\Lambda}^{5G}$. Initialize $\mathbf{\Pi} = \mathcal{M}$, $\mathbf{\Lambda}^{\mathrm{PLC}} = \emptyset$, $\mathbf{\Lambda}^{5G} = \emptyset$, $\gamma_i^{\mathrm{PLC}}(0) = \rho$, and $\gamma_i^{5G}(0) = \rho$, $\forall m_i \in \mathcal{M}$, where ρ is a predefined constant.

For $v = 1,2,\ldots,V$, **do**
  Phase 1: Initialization
  Initialize $\mathbf{\Pi} = \mathcal{M}$, $\mathbf{\Lambda}^{\mathrm{PLC}} = \emptyset$, $\mathbf{\Lambda}^{\mathrm{5G}} = \emptyset$, $\gamma_i^{\mathrm{PLC}}(\emptyset) = \rho$, and $\gamma_i^{\mathrm{5G}}(\emptyset) = \rho$.
  Phase 2: 5G and PLC preference value calculation
  Calculate $\gamma_i^{\mathrm{PLC}}(v)$ and $\gamma_i^{\mathrm{5G}}(v)$ based on (18) and (19).
  while $\mathbf{\Pi} \neq \emptyset$, **do**
    Phase 3: 5G and PLC preference list construction
    Construct $\boldsymbol{P}_i$ based on $\gamma_i^{\mathrm{PLC}}(v)$ and $\gamma_i^{\mathrm{5G}}(v)$.
    Phase 4: I-to-2 matching
    $m_i \in \mathcal{M}$ sends matching request to its most preferred communication mode based on $\gamma_i^{\mathrm{PLC}}(v)$ and $\gamma_i^{\mathrm{5G}}(v)$.
    if $|\mathbf{\Lambda}^{\mathrm{PLC}}| \leq J_1$, **then**
      $m_i \in \mathbf{\Lambda}^{\mathrm{PLC}}$ selects the PLC mode and sets the corresponding $x_i^{\mathrm{PLC}}(v) = 1$.
      Update $\mathbf{\Pi} = \mathbf{\Pi}\ \mathbf{\Lambda}^{\mathrm{PLC}}$
    end if
    if $|\mathbf{\Lambda}^{\mathrm{5G}}| \leq J_2$, **then**
      $m_i \in \mathbf{\Lambda}^{\mathrm{5G}}$ selects the 5G communication mode and sets the corresponding $x_i^{\mathrm{5G}}(v) = 1$.
      Update $\mathbf{\Pi} = \mathbf{\Pi}\ \mathbf{\Lambda}^{\mathrm{5G}}$
    end if
    Phase 5: bidding matching and preference value update
    if $|\Lambda^{\mathrm{PLC}}| > J_1$, **then**
    $m_i \in \mathbf{\Lambda}^{\mathrm{PLC}}$ starts bidding and updates $\gamma_i^{\mathrm{PLC}}(v)$ based on Eq. (20) and (22).
    if $\exists m_i \in \mathbf{\Lambda}^{\mathrm{PLC}}, \gamma_i^{\mathrm{PLC}}(v) < \gamma_i^{\mathrm{5G}}(v)$, **then**
      m_i sends matching request to the 5G communication mode and updates $\mathbf{\Lambda}^{\mathrm{PLC}} = \mathbf{\Lambda}^{\mathrm{PLC}}\ m_i$.
    end if
  end if
  if $|\mathbf{\Lambda}^{\mathrm{5G}}| > J_2$, **then**
    $m_i \in \mathbf{\Lambda}^{\mathrm{5G}}$ starts bidding and updates $\gamma_i^{\mathrm{5G}}(v)$ based on Eq. (21) and (23).
    if $\exists m_i \in \mathbf{\Lambda}^{\mathrm{5G}}, \gamma_i^{\mathrm{5G}}(v) < \gamma_i^{\mathrm{PLC}}(v)$, **then**
      m_i sends matching request to the PLC mode and updates $\mathbf{\Lambda}^{\mathrm{5G}} = \mathbf{\Lambda}^{\mathrm{5G}}\ m_i$.
    end if
  end if
  Repeat the above steps until $\mathbf{\Pi} = \emptyset$.
end while
end for

Algorithm 1. Large-timescale communication mode selection based on I-to-2 bidding matching.

3.1.2 5G and PLC preference value calculation

The preference values $\gamma_i^{\mathrm{PLC}}(v)$ and $\gamma_i^{\mathrm{5G}}(v)$ are calculated by the edge server. We utilize the historical performance to calculate the preference values $\gamma_i^{\mathrm{PLC}}(v)$ and $\gamma_i^{\mathrm{5G}}(v)$, which are represented as Eq. 18, Eq. 19, respectively. Here, Eq. 18 is considered an example. The first term of the numerator, i.e., $\gamma_i^{\mathrm{PLC}}(v-1)\left(\sum_{z=1}^{v-1} x_i^{\mathrm{PLC}}(z)+1\right)$, represents the accumulative preference value of m_i for PLC until the $(v-1)$-th epoch, while the second term of the numerator, i.e., $x_i^{\mathrm{PLC}}(v)\frac{\sum_{t=(v-1)T_0}^{vT_0}\tau_i(t)}{T_0}$, represents the average transmission delay of m_i within the v-th epoch. The denominator, i.e., $\sum_{z=1}^{v} x_i^{\mathrm{PLC}}(z)+1$, represents the total number of selecting PLC mode of m_i until the v-th epoch. Eq. 19 is defined similarly.

$$\gamma_i^{\mathrm{PLC}}(v) = \frac{\gamma_i^{\mathrm{PLC}}(v-1)\left(\sum_{z=1}^{v-1} x_i^{\mathrm{PLC}}(z)+1\right) - x_i^{\mathrm{PLC}}(v)\frac{\sum_{t=(v-1)T_0}^{vT_0}\tau_i(t)}{T_0}}{\sum_{z=1}^{v} x_i^{\mathrm{PLC}}(z)+1}, \tag{18}$$

$$\gamma_i^{\mathrm{5G}}(v) = \frac{\gamma_i^{\mathrm{5G}}(v-1)\left(\sum_{z=1}^{v-1} x_i^{\mathrm{5G}}(z)+1\right) - x_i^{\mathrm{5G}}(v)\frac{\sum_{t=(v-1)T_0}^{vT_0}\left(\tau_i(t)+\alpha C_i(t)\right)}{T_0}}{\sum_{z=1}^{v} x_i^{\mathrm{5G}}(z)+1}. \tag{19}$$

3.1.3 5G and PLC preference list construction

Denote the 5G and PLC preference list of device m_i as $\boldsymbol{P}_i$. Each device constructs the preference list by arranging its preference values $\gamma_i^{\mathrm{PLC}}(v)$ and $\gamma_i^{\mathrm{5G}}(v)$ in a descending order. The communication mode with the largest preference value is prioritized to be selected, which ranks top in the preference list.

3.1.4 I-to-2 matching

Each device $m_i \in \mathbf{\Pi}$ issues a matching request to its most preferred communication mode based on its preference list. Denote the number of devices selecting the PLC mode as $|\mathbf{\Lambda}^{\mathrm{PLC}}|$, which is the number of elements in the set $\mathbf{\Lambda}^{\mathrm{PLC}}$. Similarly, the number of devices selecting the 5G communication mode is $|\mathbf{\Lambda}^{\mathrm{5G}}|$. When $|\mathbf{\Lambda}^{\mathrm{PLC}}| \leq J_1$, devices selecting the PLC mode, i.e., $m_i \in \mathbf{\Lambda}^{\mathrm{PLC}}$, are matched successfully with the PLC mode, i.e., $x_i^{\mathrm{PLC}}(v) = 1$. Then, the devices which are successfully matched with the PLC mode are removed from the set of unmatched devices, i.e., $\mathbf{\Pi} = \mathbf{\Pi} \backslash \mathbf{\Lambda}^{\mathrm{PLC}}$. Similarly, when $|\mathbf{\Lambda}^{\mathrm{5G}}| \leq J_2$, devices selecting the 5G mode, i.e., $m_i \in \mathbf{\Lambda}^{\mathrm{5G}}$, are matched successfully with the 5G communication mode, i.e., $x_i^{\mathrm{5G}}(v) = 1$. Then, the devices which are successfully matched with the 5G mode are removed from the set of unmatched devices, i.e., $\mathbf{\Pi} = \mathbf{\Pi} \backslash \mathbf{\Lambda}^{\mathrm{5G}}$.

3.1.5 Bidding matching and preference value update

When $|\mathbf{\Lambda}^{\mathrm{PLC}}| \geq J_1$ or $|\mathbf{\Lambda}^{\mathrm{5G}}| \geq J_2$, competition of communication mode selection occurs, and C_3 or C_4 cannot be satisfied. To address the competition issues, bidding matching is proposed to iteratively reduce the preference value based on the bidding price. Moreover, the bidding price can be dynamically adjusted to enable larger preference for devices with a large queuing delay and virtual queue backlog.

To enable higher priority for devices with a larger virtual queue backlog and queuing delay, the bidding price is negatively proportional to an historical virtual queue backlog and queuing delay. The bidding prices of device m_i toward PLC and 5G modes are given by

$$p_i^{\mathrm{PLC}}(v) = \frac{\beta^{\mathrm{PLC}} \gamma_i^{\mathrm{PLC}}(v)}{\sum_{t=(v-1)T_0}^{vT_0} O_i(t)\, \tau_i^{\mathrm{que}}(t)}, \tag{20}$$

$$p_i^{\mathrm{5G}}(v) = \frac{\beta^{\mathrm{5G}} \gamma_i^{\mathrm{5G}}(v)}{\sum_{t=(v-1)T_0}^{vT_0} O_i(t)\, \tau_i^{\mathrm{que}}(t)}, \tag{21}$$

where β^{PLC} and β^{5G} denote the bidding price coefficients for the PLC and 5G communication modes, respectively. Taking (20) as an example, the numerator represents the bidding step size, and the denominator represents the historical virtual queue backlog and queuing delay.

The device m_i reduces its preference values for the PLC and 5G communication modes by subtracting the bidding prices, which are given by

$$\gamma_i^{\mathrm{PLC}}(v) = \gamma_i^{\mathrm{PLC}}(v) - p_i^{\mathrm{PLC}}(v), \tag{22}$$

$$\gamma_i^{\mathrm{5G}}(v) = \gamma_i^{\mathrm{5G}}(v) - p_i^{\mathrm{5G}}(v). \tag{23}$$

Since the bidding price is negatively related to the virtual queue backlog and queuing delay, devices with worse historical performances will have a larger preference value and higher priority to be matched.

Then, repeat *3*), *4*), and *5*) until $\mathbf{\Pi} = \emptyset$.

In *3*), i.e., the procedure of 5G and PLC preference list construction, devices reconstruct the preference list based on the updated preference values. The subtraction of bidding price lowers the preference value and changes the ranking of communication modes in the preference list. For example, device m_i which used to select PLC in the previous iteration may select 5G in the current iteration because the preference value toward PLC is reduced, and the PLC mode becomes less attractive than 5G. In this way, bidding price enforces some devices to withdraw matching, thereby resolving communication mode selection competition.

3.2 Small-timescale subchannel allocation based on many-to-many deferred acceptance matching

Based on the large-timescale optimization results of communication mode selection, the small-timescale subchannel allocation problem is decomposed into a PLC subchannel allocation subproblem and a 5G subchannel allocation subproblem, which can be solved simultaneously by the proposed many-to-many deferred acceptance matching. The objective is to minimize the weighted sum of data transmission delay and traffic cost by establishing a bilateral matching relationship between devices and subchannels. Some definitions of the algorithm put forward are described below.

Definition 1 (Bilateral preference relation): For the matching between devices and subchannels, the complete, reflective, and transitive bilateral relation between devices and subchannels, i.e.,“ $\succ$,” is expressed” through the bilateral preference relation, which indicates the extent of mutual preference. It is introduced to compare the preferences as

$$m_i \succ_{n_j} n_{j'} \Leftrightarrow \omega_{i,j}(t) > \omega_{i,j'}(t), \tag{24a}$$

$$n_j \succ_{m_i} m_{i'} \Leftrightarrow \lambda_{i,j}(t) > \lambda_{i',j}(t), \tag{24b}$$

where $\Leftrightarrow$ means equivalence. $m_i \succ_{n_j} n_j'$ means that the device m_i prefers the subchannel n_j more than the subchannel $n_{j'}$ because $\omega_{i,j'}(t)$ is smaller than the preference value $\omega_{i,j}(t)$. $n_j \succ_{m_i} m_{i'}$ means that the subchannel n_j prefers the device m_i more than the device $m_{i'}$ because $\lambda_{i',j}(t)$ is smaller than the preference value $\lambda_{i,j}(t)$.

Definition 2 (bilateral matching): The small-timescale subchannel allocation is a bilateral matching ϕ with constraints of device quota and transmission reliability, i.e.,

$$\phi(m_i) \subseteq \mathcal{N} \quad \text{and} \quad |\phi(m_i)| \leq q_m, \forall n_j \in \mathcal{N}, \tag{25a}$$

$$\phi(n_j) \subseteq \mathcal{M} \quad \text{and} \quad |\phi(n_j)| \leq 1, \forall m_i \in \mathcal{M}, \tag{25b}$$

$$\phi(m_i) \subseteq \mathcal{N} \quad \text{and} \quad SINR_{i,j}(t) \geq SINR_{min}, \forall m_i \in \mathcal{M}, \tag{25c}$$

$$n_j \in \phi(m_i) \Leftrightarrow m_i \in \phi(n_j), \tag{25d}$$

where (25a) ensures that at most q_m subchannels can be allocated to m_i. (25b) indicates that each subchannel can be allocated to at most one device. (25c) indicates that the SINR of the subchannel allocated to m_i needs to meet the requirement of transmission reliability. (25d) means that the subchannel n_j is matched to the device m_i if m_i is matched to n_j.

Definition 3 (stable matching): If the matching ϕ satisfies individual rationality criteria and is not disrupted by any pair, it is deemed to be stable.

Based on the above definitions, we propose the small-timescale subchannel allocation algorithm based on many-to-many deferred acceptance matching. Algorithm 2 encapsulates the detailed procedural steps for implementation.

3.2.1 Grouping and initialization

According to the large-timescale optimization results of communication mode selection, devices are divided into two groups. Among them, the devices that select the PLC mode belong to the set $\mathcal{M}^{\mathrm{PLC}}$, and the devices that select the 5G communication mode belong to the set $\mathcal{M}^{\mathrm{5G}}$. Define $\Theta_i(t)$ as the set of PLC subchannels that are currently matched with m_i. Denote $|\Theta_i(t)|$ as the size of $\Theta_i(t)$, i.e., the number of subchannels allocated to m_i. Initialize $y_{i,j}(t) = 0$ and $\Theta_i(t) = \emptyset$.

3.2.2 Bilateral preference value calculation

According to the grouping results, $\forall m_i \in \mathcal{M}^{\mathrm{PLC}}$, the preference values of m_i toward the PLC subchannel n_j are calculated by the edge

for $t=(v-1)T_0+1,(v-1)T_0+2,\ldots,vT_0$ **do**
  Phase 1: Grouping and initialization
  Initialize $\Theta_i(t)=\emptyset$ and $y_{i,j}=0$.
  Phase 2: Bilateral preference value calculation
  $\forall m_i \in \mathcal{M}$ calculates its preference value toward n_j based on (26) and (28).
  $\forall n_j \in \mathcal{N}$ calculates its preference value toward m_i based on (27) and (29).
  Phase 3: Bilateral partial preference list construction
  m_i and n_j construct $\mathcal{F}_i^D$ and $\mathcal{F}_j^C$ based on C_7 and large-timescale optimization results.
  Phase 4: Device and 5G subchannel bilateral deferred acceptance matching
  $\forall m_i \in \mathcal{M}^{5G}$ sends matching proposals to its most preferred $(q_m-|\Theta_i(t)|)$ 5G subchannel in $\mathcal{F}_i^D$.
  for $n_j, j=J_1+1,\ldots,J$ **do**
    if C_6 is satisfied **then**
      Derive stable matching between devices and 5G subchannels.
    end if
    if C_6 is not satisfied **then**
      if $y_{i,j}=0$ **then**
        n_j selects the device m_i with the largest preference rejects the other devices and sets $y_{i,j}(t)=1$.
      else
        n_j compares $m_{i'}$ with m_i and selects the device with the largest preference value.
        n_j rejects the other devices and renews the tentative matching relationship.
      end if
    end if
    Remove the devices which are temporarily matched with 5G subchannels from $\mathcal{F}_j^C$. Remove the 5G subchannels which have rejected m_i from $\mathcal{F}_i^D$.
    Repeat the above steps until no 5G subchannel remains.
  end for
  Phase 5: Device and PLC subchannel bilateral deferred acceptance matching
  Perform the bilateral deferred acceptance matching between devices and PLC subchannel similarly.
end for

Algorithm 2. Small-timescale subchannel allocation based on many-to-many deferred acceptance matching.

server, which is defined as the reciprocal of the data transmission delay, i.e.,

$$\omega_{i,j}(t)=\frac{x_i^{\mathrm{PLC}}(v)}{\tau_i(t)},\quad j=1,\ldots,J_1. \tag{26}$$

Considering higher priority for devices with a large virtual queue backlog and queuing delay, the preference value of the PLC subchannel n_j toward m_i is defined as the product of the virtual queue backlog and queuing delay, which is given by

$$\lambda_{i,j}(t)=x_i^{\mathrm{PLC}}(v)\,O_i(t)\,\tau_i^{\mathrm{que}}(t),\quad j=1,\ldots,J_1. \tag{27}$$

Similarly, $\forall m_i \in \mathcal{M}^{5G}$, combined with the extra traffic cost of using 5G subchannels, the preference value of m_i toward 5G subchannel n_j is defined as

$$\omega_{i,j}(t)=\frac{x_i^{5G}(v)}{\tau_i(t)+\alpha C_i(t)}, j=J_1,\ldots,J. \tag{28}$$

The preference value of the 5G subchannel n_j toward m_i is given by

$$\lambda_{i,j}(t)=x_i^{5G}(v)\,O_i(t)\,\tau_i^{\mathrm{que}}(t), j=J_1,\ldots,J. \tag{29}$$

3.2.3 Bilateral partial preference list construction

Unlike the large-timescale matching in communication mode selection, the preference list of subchannel allocation is partial because subchannels which cannot meet the minimum SINR requirement are removed from the preference list. Assuming that device m_i selects the 5G communication mode, the set of available 5G subchannels for m_i is defined as $\mathcal{N}_i(t)=\left\{n_j|n_j\in\mathcal{N}, SINR_{i,j}(t)\geq SINR_{\min}, j=J_1+1,\ldots,J\right\}$.

Then, m_i constructs the partial preference list of 5G subchannels, i.e., $\mathcal{F}_i^D$, by sorting the preference values of 5G subchannels of set $\mathcal{N}_i(t)$ in descending order. Next, each 5G subchannel constructs the preference list of devices based on (29). The partial preference list of the subchannel n_j is defined as $\mathcal{F}_j^C$. The bilateral preference lists between devices and PLC subchannels are constructed similarly.

3.2.4 Device and 5G subchannel bilateral deferred acceptance matching

Bilateral deferred acceptance is used to derive a stable matching between devices and 5G subchannels.

TABLE 2 Simulation parameters (Seo, 2012).

Parameter	Value	Parameter	Value
J_1, J_2	1000, 280	I	100
q_m	100	$R_j^{\max}$	8 bits/symbol
T	100	$P_{i,j}(t)$	−17 dBm
V	10	T_0	10
τ	1 s	$e^{5G}(v)$	0.4 $/Gbits
ρ	1	$SINR_{\min}$	12.3 dB
N_s	14,000 symbols/s	α	200
N_0	−114 dBm	P_e	10^{-7}
v	1.4	η	−0.791
θ	10^{-4}	μ	[1.2,2.6]

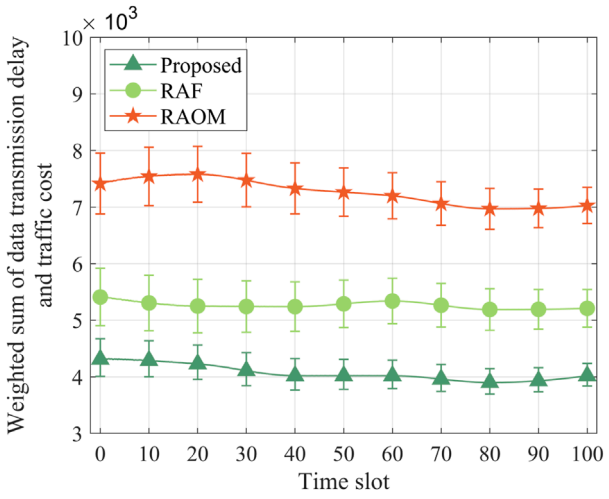

FIGURE 3
Weighted sum of data transmission delay and traffic cost *versus* time slot (I = 100).

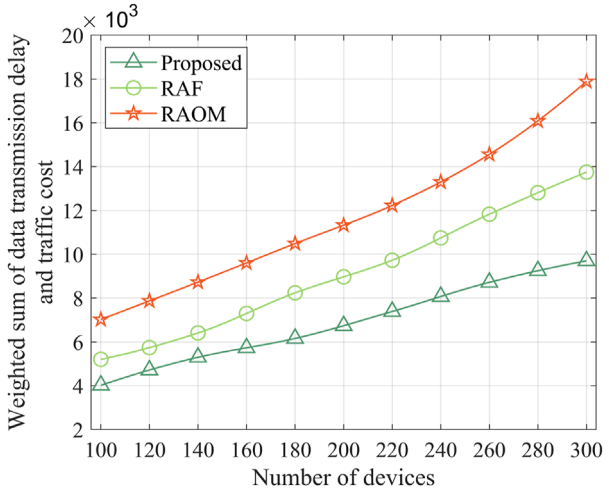

FIGURE 4
Weighted sum of data transmission delay and traffic cost *versus* the number of devices.

Step 1: $m_i \in \mathcal{M}^{5G}$ sends matching proposals to its most preferred $(q_m - |\Theta_i(t)|)$ 5G subchannels in its preference list $\mathcal{F}_i^D$.

Step 2: Each 5G subchannel, i.e., n_j, $j = J_1 + 1, \ldots, J$, calculates the total number of received matching proposals. If the matching proposals received by all 5G subchannels meet the constraint C_6, then a stable matching between devices and 5G subchannels is derived. The bilateral deferred acceptance matching is terminated. Otherwise, if the constraint C_6 is not satisfied, execute Step 3.

Step 3: Assume that n_j receives more than one matching proposals. If n_j has not established a tentative matching relationship with any device in previous iterations, it selects the device with the largest preference, e.g., m_i, and rejects the other devices. Then, a tentative matching relationship is established between n_j and m_i, i.e., $y_{i,j}(t) = 1$.

If n_j has established a tentative matching relationship with some device in previous iterations, e.g., $m_{i'}$, it compares $m_{i'}$ with m_i and selects the device with the largest preference value. Next, it rejects other devices and renews the tentative matching relationship. Therefore, devices which have been matched with subchannels in previous iterations may get rejected in later iterators if better matching candidate appears, which stands for the meaning of deferred acceptance.

Step 4: The devices which are temporarily matched with 5G subchannels are removed from the set $\mathcal{F}_j^C$. Meanwhile, the 5G subchannels which have rejected m_i are removed from the set $\mathcal{F}_i^D$. Then, go back to Step 1 and reperform bilateral matching for the rejected devices until no 5G subchannel remains.

3.2.5 Device and PLC subchannel bilateral deferred acceptance matching

The bilateral deferred acceptance matching between devices and PLC subchannels is performed similarly as that of 5G. The iterative process between n_j and m_i is repeated until no PLC subchannel remains. The proposed algorithm divides devices into two groups based on the large-timescale communication mode selection result and allows parallel implementation of two matchings. This dramatically reduces matching complexity and convergence performance compared to existing approaches.

4 Simulation results

Within this segment, the efficacy of the algorithm put forward is assessed via simulation-based analysis. An IoT-empowered distribution energy dispatch scenario containing 10 IoT devices is set. The quota of subchannel allocation q_m is set as 10. There are 128 orthogonal subchannels, including 100 PLC subchannels and 28 5G subchannels. The alpha steady-state function is used to describe electromagnetic interference. Table 2 presents the parameters used

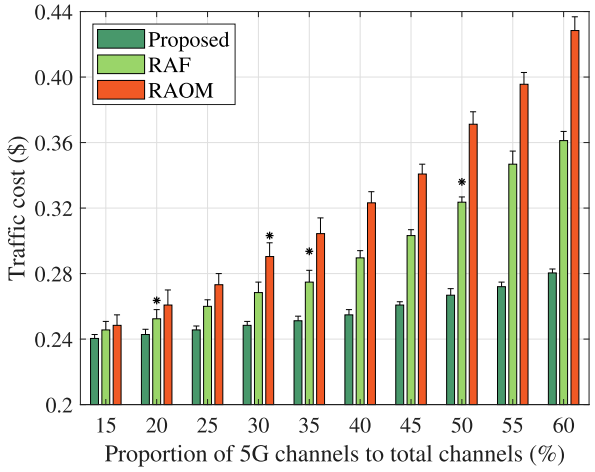

FIGURE 5
Traffic cost *versus* proportion of the 5G subchannel.

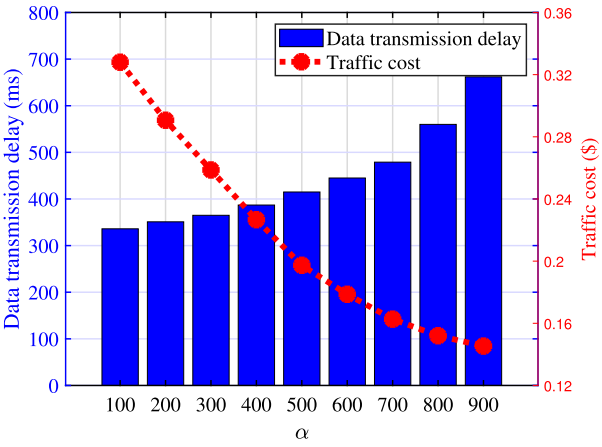

FIGURE 6
Data transmission delay and traffic cost *versus* α.

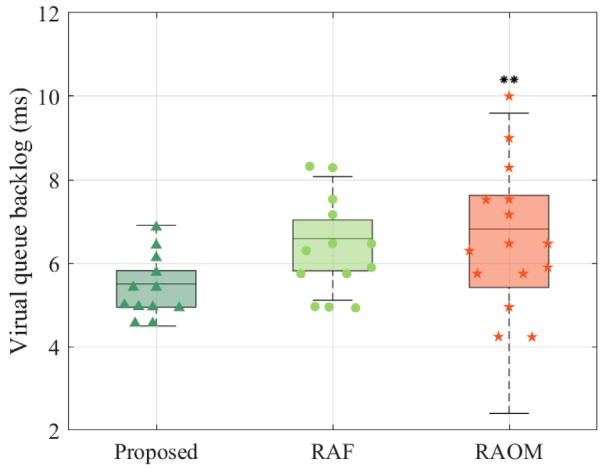

FIGURE 7
Box plots of the virtual queue backlog.

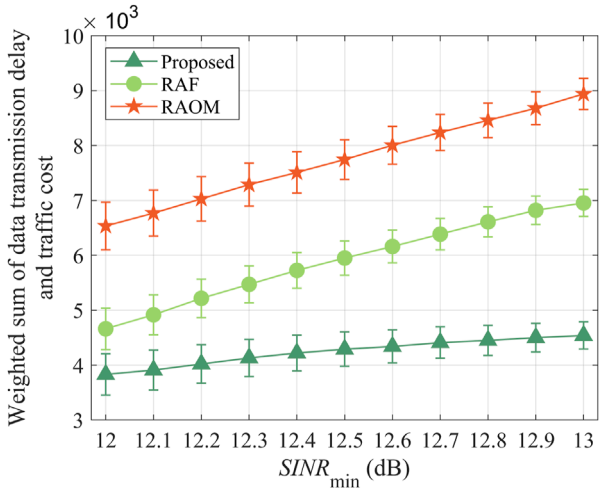

FIGURE 8
Weighted sum of data transmission delay and traffic cost *versus* $SINR_{min}$.

for the simulation (Liao et al., 2020; Zhang P. et al., 2023). Two existing algorithms are compared with the algorithm put forward. The first algorithm is the resource allocation scheme based on the fire algorithm (RAF), which minimizes the weighted sum of transmission delay and traffic cost and ignores the large-timescale optimization of communication mode selection (Liu et al., 2019). The second algorithm is the resource allocation algorithm based on one-to-many matching (RAOM), which neglects the traffic cost optimization (Yuan et al., 2019). Both comparison algorithms do not consider the long-term average queuing delay constraint.

Figure 3 shows the weighted sum of data transmission delay and traffic cost *versus* time slot. With the device number escalating from 100 to 300, the weighted sum performances of the proposed algorithm, RAF, and RAOM exhibit enhancements of 20.82%, 53.78%, and 37.47%, respectively. The algorithm put forward considers the optimization of the communication mode selection and subchannel allocation in a multi-timescale. In a large timescale, by updating the bidding price, the proposed algorithm resolves the conflicts among devices. In a small timescale, the proposed algorithm calculates the preference value based on the data transmission delay, traffic cost, virtual queue backlog, and queuing delay. The proposed algorithm constructs the partial preference list, according to the data transmission reliability requirement, and executes the grouping matching based on the large-timescale decisions. This effectively reduces the complexity of matching iteration and improves the weighted sum of data transmission delay and traffic cost while satisfying the long-term average queuing delay constraint. RAF ignores the large-timescale communication mode selection, leading to the high complexity and worse weighted sum performance. RAOM does not consider traffic cost optimization, and its performance is the worst.

Figure 4 shows the weighted sum of data transmission delay and traffic cost *versus* the number of devices. With the device number escalating from 10 to 110, the weighted sum performances of the proposed algorithm, RAF, and RAOM exhibit

enhancements of 20.82%, 53.78%, and 37.47%, respectively. When $I = 110$, compared with RAF and RAOM, the proposed algorithm reduces the weighted sum performance by 33.13% and 53.65%, respectively. The algorithm put forward addresses the conflicts through the dynamic bidding in a large timescale and the bilateral deferred acceptance matching in a small timescale, which can achieve the stable two-layer iterative matching strategies among devices.

Figure 5 shows the traffic cost *versus* proportion of the 5G subchannel. As the proportion of the 5G subchannel increases from 15% to 60%, the traffic cost of the proposed algorithm increases at a slower pace compared to that of RAF and RAOM. When the proportion of 5G subchannel is 60%, the traffic cost of the proposed algorithm is 34.03% and 53.35% lower than those of RAF and RAOM, respectively. The proposed algorithm considers the trade-off between data transmission delay and traffic cost, avoiding the problem of high traffic cost due to the excessive selection of 5G channels when the 5G subchannel number is high.

Figure 6 shows the data transmission delay and traffic cost *versus* α. The simulation result shows that the traffic cost increases gradually with α, while the data transmission delay decreases contrarily. When α increases from 100 to 900, the data transmission delay is reduced by 95.25%, and the traffic cost is increased by 55.45%. The increase in α makes the proposed algorithm tend to optimize the transmission delay. Therefore, a dynamic tradeoff is achieved between data transmission delay and traffic cost by adaptively adjusting α in the proposed algorithm.

Figure 7 shows the box plots of the virtual queue backlog. Compared with RAF and RAOM, the proposed algorithm reduces the median virtual queue backlog by 23.73% and 30.08%, respectively. The proposed algorithm transforms the long-term constraint of average queuing delay into the stability of virtual queue based on Lyapunov optimization. Moreover, it considers the virtual queue of queuing delay into the preference value calculation and effectively solves the competition problem among devices.

Figure 8 shows the weighted sum of data transmission delay and traffic cost *versus* $SINR_{\min}$. As $SINR_{\min}$ increases, the weighted sum performances of the three algorithms gradually increase. The proposed algorithm achieves smallest increment. This is due to the decrease in available channels caused by the increase in $SINR_{\min}$, resulting in an overall performance degradation. The proposed algorithm can optimize the communication resource allocation strategies based on the alternately iterative matching between the large timescale and small timescale. In addition, the proposed algorithm enhances the optimality of matching through the bidding and deferred acceptance mechanisms.

5 Conclusion

In this paper, we addressed the joint minimization problem of data transmission delay and traffic cost. The delay and cost-balanced communication resource management algorithm based on two-layer iterative matching is proposed to satisfy the constraints of the subchannel allocation number, subchannel allocation quota, data transmission reliability, and long-term average queuing delay by jointly optimizing the large-timescale communication mode selection and small-timescale subchannel allocation. Compared with the RAF and RAOM algorithm, the proposed algorithm reduces the weighted sum of data transmission delay and traffic cost by 43.22% and 22.13%, respectively. Particularly, the proposed algorithm can efficiently guarantee the long-term average queuing delay constraint. Compared with RAF and RAOM, the proposed algorithm reduces the median virtual queue backlog by 23.73% and 30.08% and achieves the best queuing delay performance.

The large-scale access of IoT devices causes an explosion of data for distribution energy dispatch. Limited computing resources of the edge server cannot meet the data processing demands. A potential solution is to combine edge computing with cloud computing, thereby constructing a cloud-edge collaborative computing framework to improve the data processing capacity. However, this increases the optimization complexity of communication resource allocation. How to reasonably allocate computing resources to meet the data processing requirements with different service priority is also an open issue. Therefore, future work will focus on the joint optimization of cloud-edge collaborative communication and computing resources to further improve the data processing performance for IoT-empowered distribution grid energy dispatch.

Data availability statement

The original contributions presented in the study are included in the article/Supplementary Material; further inquiries can be directed to the corresponding author.

Author contributions

ZS: conceptualization, formal analysis, funding acquisition, investigation, methodology, software, validation, writing–original draft, and writing–review and editing.

Funding

The author(s) declare that financial support was received for the research, authorship, and/or publication of this article. This work was supported by the China Southern Power Grid Technology Project under the grant number 03600KK52220019 (GDKJXM20220253).

Conflict of interest

Author ZS was employed by Guangdong Power Grid Co., Ltd.

The authors declare that this study received funding from China Southern Power Grid Technology Project. The funder had the following involvement in the study: study design, collection, interpretation of data, the writing of this article, and the decision to submit it for publication.

Publisher's note

References

Adnan, M., Tariq, M., Zhou, Z., and Poor, H. (2019). Load flow balancing and transient stability analysis in renewable integrated power grids. *Int. J. Electr. Power Energy Syst.* 104, 744–771. funding Information: This work was supported in part by the U.S. National Science Foundation under Grants DMS-1736417 and ECCS-1824710. Publisher Copyright: © 2018 Elsevier Ltd. doi:10.1016/j.ijepes.2018.06.037

Ali, M., Adnan, M., Tariq, M., and Poor, H. V. (2021). Load forecasting through estimated parametrized based fuzzy inference system in smart grids. *IEEE Trans. Fuzzy Syst.* 29 (1), 156–165. doi:10.1109/tfuzz.2020.2986982

Bigdeli, M., Abolhassani, B., Farahmand, S., and Tellambura, C. (2023). Offline and real-time deadline-aware scheduling and resource allocation algorithms favoring big data transmission over cognitive CRANs. *IEEE Access* 11 (99), 67755–67778. doi:10.1109/access.2023.3288996

Chagnon, M. (2019). Optical communications for short reach. *J. Light. Technol.* 37 (8), 1779–1797. doi:10.1109/jlt.2019.2901201

Csercsik, D., and Jorswieck, E. A. (2023). Preallocation-based combinatorial auction for efficient fair channel assignments in multi-connectivity networks. *IEEE Trans. Wirel. Commun.* 22 (11), 8407–8422. doi:10.1109/twc.2023.3263041

Dewa, G. R. R., Alfathani, A. S., Park, C., and Sohn, I. (2021). Distributed channel assignment for ultra-dense wireless networks using belief propagation. *IEEE Access* 9, 117040–117051. doi:10.1109/access.2021.3105717

Ding, G., Yuan, J., Yu, G., and Jiang, Y. (2022). Two-timescale resource management for ultrareliable and low-latency vehicular communications. *IEEE Trans. Commun.* 70 (5), 3282–3294. doi:10.1109/tcomm.2022.3162366

Do, L. P., and Lehnert, R. (2011). "A channel allocation protocol for providing fairness between users in multi-cell PLC networks," in 2011 IEEE International Symposium on Power Line Communications and Its Applications, Udine, Italy, 03-06 April 2011, 1–6.

Fizza, K., Jayaraman, P. P., Banerjee, A., Auluck, N., and Ranjan, R. (2023). IoT-Qwatch: a novel framework to support the development of quality-aware autonomic IoT applications. *IEEE Internet Things J.* 10 (20), 17666–17679. doi:10.1109/jiot.2023.3278411

Gu, B., Chen, W., Alazab, M., Tan, X., and Guizani, M. (2022). Multiagent reinforcement learning-based semi-persistent scheduling scheme in C-V2X mode 4. *IEEE Trans. Veh. Technol.* 71 (11), 12044–12056. doi:10.1109/tvt.2022.3189019

Gu, B., Zhang, X., Lin, Z., and Alazab, M. (2021). Deep multiagent reinforcement-learning-based resource allocation for internet of controllable things. *IEEE Internet Things J.* 8 (5), 3066–3074. doi:10.1109/jiot.2020.3023111

Guo, C., He, W., and Li, G. Y. (2021). Optimal fairness-aware resource supply and demand management for mobile edge computing. *IEEE Wirel. Commun. Lett.* 10 (3), 678–682. doi:10.1109/lwc.2020.3046023

Han, X., Li, Z., and Xie, Z. (2023). Two-step random access optimization for 5G-and-beyond LEO satellite communication system: a TD3-based MsgA channel allocation strategy. *IEEE Commun. Lett.* 27 (6), 1570–1574. doi:10.1109/lcomm.2023.3266777

Huang, H., Li, Z., Sampath, L. P. M. I., Yang, J., Nguyen, H. D., Gooi, H. B., et al. (2023). Blockchain-enabled carbon and energy trading for network-constrained coal mines with uncertainties. *IEEE Trans. Sustain. Energy* 14 (3), 1634–1647. doi:10.1109/tste.2023.3240203

Huang, Q., Jia, Q.-S., and Guan, X. (2015). "Multi-timescale optimization between distributed wind generators and electric vehicles in microgrid," in 2015 IEEE International Conference on Automation Science and Engineering (CASE), Gothenburg, Sweden, 24-28 August 2015, 671–676.

Huang, Y., Zhao, C., Tang, B., and Fu, H. (2022). Beacon synchronization-based multi-channel with dynamic time slot assignment method of wsns for mechanical vibration monitoring. *IEEE Sensors J.* 22 (13), 13659–13667. doi:10.1109/jsen.2022.3165811

Islam, M. T., Taha, A.-E. M., Akl, S., and Abu-Elkheir, M. (2016). "A stable matching algorithm for resource allocation for underlaying device-to-device communications," in 2016 IEEE International Conference on Communications (ICC), Kuala Lumpur, Malaysia, 22-27 May 2016, 1–6.

Leng, R., Li, Z., and Xu, Y. (2023). Two-stage stochastic programming for coordinated operation of distributed energy resources in unbalanced active distribution networks with diverse correlated uncertainties. *J. Mod. Power Syst. Clean Energy* 11 (1), 120–131. doi:10.35833/mpce.2022.000510

Li, X., Chen, G., Wu, G., Sun, Z., and Chen, G. (2023a). Research on multi-agent d2d communication resource allocation algorithm based on A2C. *ELECTRONICS* 12 (2), 360. doi:10.3390/electronics12020360

Li, Z., Xu, Y., Wang, P., and Xiao, G. (2023b). Restoration of multi energy distribution systems with joint district network recon figuration by a distributed stochastic programming approach. *IEEE Trans. Smart Grid*, 1. doi:10.1109/tsg.2023.3317780

Liao, H., Zhou, Z., Jia, Z., Shu, Y., Tariq, M., Rodriguez, J., et al. (2023a). Ultra-low AoI digital twin-assisted resource allocation for multi-mode power IoT in distribution grid energy management. *IEEE J. Sel. Areas Commun.* 41 (10), 3122–3132. doi:10.1109/jsac.2023.3310101

Liao, H., Zhou, Z., Liu, N., Zhang, Y., Xu, G., Wang, Z., et al. (2023b). Cloud-edge-device collaborative reliable and communication-efficient digital twin for low-carbon electrical equipment management. *IEEE Trans. Industrial Inf.* 19 (2), 1715–1724. doi:10.1109/tii.2022.3194840

Liao, H., Zhou, Z., Zhao, X., Zhang, L., Mumtaz, S., Jolfaei, A., et al. (2020). Learning-based context-aware resource allocation for edge-computing-empowered industrial IoT. *IEEE Internet Things J.* 7 (5), 4260–4277. doi:10.1109/jiot.2019.2963371

Lin, D., Zuo, P., Peng, T., Qian, R., and Wang, W. (2023). Energy-efficient UAV-based IoT communications with wifi suppression in 5 GHz ISM bands. *IEEE Trans. Veh. Technol.* 72 (2), 2024–2039. doi:10.1109/tvt.2022.3211259

Liu, H., Yan, B., and Zhao, R. (2019). Resource allocation scheme for D2D communication based on fireworks algorithm. *Comput. Eng. Appl.* 55 (8), 86–91. doi:10.3778/j.issn.1002-8331.1801-0251

Liu, Y., Yu, W., Rahayu, W., and Dillon, T. (2023). An evaluative study on IoT ecosystem for smart predictive maintenance (IoT-SPM) in manufacturing: multiview requirements and data quality. *IEEE Internet Things J.* 10 (13), 11160–11184. doi:10.1109/jiot.2023.3246100

López, G., Matanza, J., De La Vega, D., Castro, M., Arrinda, A., Moreno, J. I., et al. (2019). The role of power line communications in the smart grid revisited: applications, challenges, and research initiatives. *IEEE Access* 7 (99), 117346–117368. doi:10.1109/access.2019.2928391

Meshgi, H., Zhao, D., and Zheng, R. (2017). Optimal resource allocation in multicast device-to-device communications underlaying LTE networks. *IEEE Trans. Veh. Technol.* 66 (9), 8357–8371. doi:10.1109/tvt.2017.2691470

Ning, Z., Wang, X., Rodrigues, J. J. P. C., and Xia, F. (2019). Joint computation offloading, power allocation, and channel assignment for 5G-enabled traffic management systems. *IEEE Trans. Industrial Inf.* 15 (5), 3058–3067. doi:10.1109/tii.2019.2892767

Pal, P., Parvathy, A. K., Devabalaji, K. R., Antony, S. J., Ocheme, S., Babu, T. S., et al. (2021). IoT-based real time energy management of virtual power plant using PLC for transactive energy framework. *IEEE Access* 9, 97643–97660. doi:10.1109/access.2021.3093111

Qian, P., Huynh, V. S. H., Wang, N., Anmulwar, S., Mi, D., and Tafazolli, R. R. (2022). Remote production for live holographic teleportation applications in 5G networks. *IEEE Trans. Broadcast.* 68 (2), 451–463. doi:10.1109/tbc.2022.3161745

Ruby, R., Yang, H., de Figueiredo, F. A. P., Huynh-The, T., and Wu, K. (2023). Energy-efficient multiprocessor-based computation and communication resource allocation in two-tier federated learning networks. *IEEE Internet Things J.* 10 (7), 5689–5703. doi:10.1109/jiot.2022.3153996

Safdar Malik, T., Razzaq Malik, K., Afzal, A., Ibrar, M., Wang, L., Song, H., et al. (2023). RL-IoT: reinforcement learning-based routing approach for cognitive radio-enabled IoT communications. *IEEE Internet Things J.* 10 (2), 1836–1847. doi:10.1109/jiot.2022.3210703

Schwung, D., Yuwono, S., Schwung, A., and Ding, S. X. (2023). PLC-informed distributed game theoretic learning of energy-optimal production policies. *IEEE Trans. Cybern.* 53 (9), 5424–5435. doi:10.1109/tcyb.2022.3179950

Seo, B. (2012). Sinr lower bound based multiuser detector for uplink MC-CDMA systems with residual frequency offset. *IEEE Commun. Lett.* 16 (10), 1612–1615. doi:10.1109/lcomm.2012.090312.121158

Sezer, A. D., and Gezici, S. (2016). Average capacity maximization via channel switching in the presence of additive white Gaussian noise channels and switching delays. *IEEE Trans. Wirel. Commun.* 15 (9), 6228–6243. doi:10.1109/twc.2016.2582150

Tariq, M., Adnan, M., Srivastava, G., and Poor, H. V. (2020). Instability detection and prevention in smart grids under asymmetric faults. *IEEE Trans. Industry Appl.* 56 (4), 1–4520. doi:10.1109/tia.2020.2964594

Wang, K., Fang, F., Costa, D. B. D., and Ding, Z. (2021). Sub-channel scheduling, task assignment, and power allocation for OMA-based and NOMA-based MEC systems. *IEEE Trans. Commun.* 69 (4), 2692–2708. doi:10.1109/tcomm.2020.3047440

Wang, X., Umehira, M., Akimoto, M., Han, B., and Zhou, H. (2023a). Green spectrum sharing framework in B5G era by exploiting crowdsensing. *IEEE Trans. Green Commun. Netw.* 7 (2), 916–927. doi:10.1109/tgcn.2022.3186282

Wang, Y., Chen, K.-C., Gong, Z., Cui, Q., Tao, X., and Zhang, P. (2023b). Reliability-guaranteed uplink resource management in proactive mobile network for minimal latency communications. *IEEE Trans. Wirel. Commun.* 22 (8), 5018–5030. doi:10.1109/twc.2022.3231319

Wang, Y., Chen, M., Huang, N., Yang, Z., and Pan, Y. (2018). Joint power and channel allocation for D2D underlaying cellular networks with rician fading. *IEEE Commun. Lett.* 22 (12), 2615–2618. doi:10.1109/lcomm.2018.2875689

Xiang, H., Yang, Y., He, G., Huang, J., and He, D. (2022). Multi-agent deep reinforcement learning-based power control and resource allocation for D2D communications. *IEEE Wirel. Commun. Lett.* 11 (8), 1659–1663. doi:10.1109/lwc.2022.3170998

Xu, Y., Liu, Z., Huang, C., and Yuen, C. (2021). Robust resource allocation algorithm for energy-harvesting-based D2D communication underlaying UAV-assisted networks. *IEEE Internet Things J.* 8 (23), 17161–17171. doi:10.1109/jiot.2021.3078264

Yao, Y., Gu, B., Su, Z., and Guizani, M. (2023). Mvstgn: a multi-view spatial-temporal graph network for cellular traffic prediction. *IEEE Trans. Mob. Comput.* 22 (5), 2837–2849. doi:10.1109/tmc.2021.3129796

Yu, H., Zhou, Z., Jia, Z., Zhao, X., Zhang, L., and Wang, X. (2021). Multi-timescale multi-dimension resource allocation for NOMA-edge computing-based power IoT with massive connectivity. *IEEE Trans. Green Commun. Netw.* 5 (3), 1101–1113. doi:10.1109/tgcn.2021.3076582

Yuan, Q., Zhao, R., and Yan, B. (2019). Resource allocation algorithm based on one-to-many matching in hierarchical heterogeneous networks. *Comput. Eng. Des.* 40 (2), 341–345. doi:10.16208/j.issn1000-7024.2019.02.008

Zhang, P., Chen, N., Xu, G., Kumar, N., Barnawi, A., Guizani, M., et al. (2023b). Multi-target-aware dynamic resource scheduling for cloud-fog-edge multi-tier computing network. *IEEE Trans. Intelligent Transp. Syst.* (99), 1–13. doi:10.1109/tits.2023.3330419

Zhang, S., Bao, S., Chi, K., Yu, K., and Mumtaz, S. (2023a). DRL-based computation rate maximization for wireless powered multi-AP edge computing. *IEEE Trans. Commun.* (99), 1. doi:10.1109/TCOMM.2023.3325905

Zhou, H., Wang, X., Umehira, M., Han, B., and Zhou, H. (2023a). Energy efficient beamforming for small cell systems: a distributed learning and multicell coordination approach. *ACM Trans. Sen. Netw.Just Accept*.

Zhou, L., Chen, X., Hong, M., Jin, S., and Shi, Q. (2021). Efficient resource allocation for multi-UAV communication against adjacent and co-channel interference. *IEEE Trans. Veh. Technol.* 70 (10), 10222–10235. doi:10.1109/tvt.2021.3104279

Zhou, P., Xu, J., Wang, W., Jiang, C., Wang, K., and Hu, J. (2020). Human-behavior and QoE-aware dynamic channel allocation for 5G networks: a latent contextual bandit learning approach. *IEEE Trans. Cognitive Commun. Netw.* 6 (2), 436–451. doi:10.1109/tccn.2020.2969631

Zhou, Z., Chen, X., Liao, H., Gan, Z., Xiao, F., Tu, Q., et al. (2023b). Collaborative learning-based network resource scheduling and route management for multi-mode green IoT. *IEEE Trans. Green Commun. Netw.* 7 (2), 928–939. doi:10.1109/tgcn.2022.3187463

Zhou, Z., Jia, Z., Liao, H., Lu, W., Mumtaz, S., Guizani, M., et al. (2022). Secure and latency-aware digital twin assisted resource scheduling for 5G edge computing-empowered distribution grids. *IEEE Trans. Industrial Inf.* 18 (7), 4933–4943. doi:10.1109/tii.2021.3137349

Zhou, Z., Wan, Y., Cui, Q., Yu, K., Mumtaz, S., Yang, C.-N., et al. (2024). Blockchain-based secure and efficient secret image sharing with outsourcing computation in wireless networks. *IEEE Trans. Wirel. Commun.* 23 (1), 423–435. doi:10.1109/twc.2023.3278108

Zhou, Z., Yang, X., and Xu, C. (2016). "Performance evaluation of multi-antenna based M2M communications for substation monitoring," in 2016 International Conference on Information and Communication Technology Convergence (ICTC), Jeju, Korea (South), 19-21 October 2016, 97–102.

Zhu, X., Ma, F., Ding, F., Guo, Z., Yang, J., and Yu, K. (2024). A low-latency edge computation offloading scheme for trust evaluation in finance-level artificial intelligence of things. *IEEE Internet Things J.* 11 (1), 114–124. doi:10.1109/jiot.2023.3297834